

W and Z Boson Production at Hadron Colliders

C. Hays

Department of Physics, University of Oxford, Oxford OX1 3RH, United Kingdom

The electroweak theory has been tested to high precision, with measurements probing its predictions at the loop level. The current generation of particle accelerators will produce enough W and Z bosons through hadron collisions to significantly improve the accuracy of these measurements. I review the issues related to such production, with particular emphasis on associated uncertainties on the W boson mass, which has now been measured more precisely at the Tevatron than at the Large Electron Positron collider.

1. Introduction

The electroweak theory is highly overconstrained, with three fundamental parameters at tree level [1] and more than a dozen precise measurements of quantities derived from these parameters [2]. The experimental precision of these measurements, typically at the 0.1% level, is sufficient to probe for loop interactions of both observed and unobserved particles.

Ongoing and future measurements at the Fermilab Tevatron and the Large Hadron Collider (LHC) will improve the accuracy of several quantities at the loop level. The mixing angle between the electromagnetic and weak symmetries, accessed through forward-backward lepton asymmetries, could have a reduced uncertainty from the full Tevatron data set [3]. The W boson mass and width have been measured most precisely by the DØ [4] and CDF [5] experiments, respectively, with accuracies that will significantly improve with the larger available data sets. The combined Tevatron top-quark mass measurement has a relative precision of 0.75% [6].

Of these measurements, the W boson mass has the greatest potential in the near term to significantly tighten constraints on unobserved particles [5]. The combination of existing measurements gives $m_W = 80.399 \pm 0.023$ GeV [7], and future CDF and DØ measurements using data already collected will be at least this precise. Including predictions from the LHC, hadron-collider measurements expect < 10 MeV precision [8], or about a factor of three reduction of the current uncertainty.

A reduction of m_W uncertainty will directly constrain the properties of new particles. The tree-level prediction $m_W = 79.964 \pm 0.005$ GeV is more than 18σ from the measured value. An important loop correction arises from the top-bottom loop, due to the large mass difference $m_t - m_b$, with the correction proportional to m_t^2 [9]. The correction arising from Higgs boson loops is proportional to $\ln m_H$. Table I shows the shift in m_W due to a doubling of m_H and to $+1\sigma$ shifts in several inputs to m_W [5, 10].

Given the ongoing and potential constraints from measurements of m_W , I focus on the status of experimental and theoretical uncertainties on this measurement at hadron colliders.

Table I The m_W shift due to a factor of two change in m_H , or $+1\sigma$ shifts in the input parameters m_t , m_Z , and α_{EM} [5, 10].

Parameter Shift	m_W Shift (MeV/ c^2)
$\Delta \ln m_H = +0.693$	-41.3
$\Delta m_t = +1.3$ GeV/ c^2	7.9
$\Delta \alpha_{EM}(Q = m_Z c^2) = +0.00035$	-6.2
$\Delta m_Z = +2.1$ MeV/ c^2	2.6

2. W and Z Boson Production

There are many components of W and Z boson production at the Tevatron that enter into the m_W measurement (Fig. 1 [5]). The interacting partons have a fraction x of the (anti)proton's momenta, with the relative fractions determining the boson's longitudinal momentum. Initial-state radiation (ISR) of gluons or photons can give the boson a transverse boost $p_T^{W(Z)}$. The boson decay is governed by the lepton electroweak charges, and spin correlations with the QCD ISR affect the decay angles. Finally, final-state radiation reduces the momentum of the charged lepton(s), affecting the inferred boson mass.

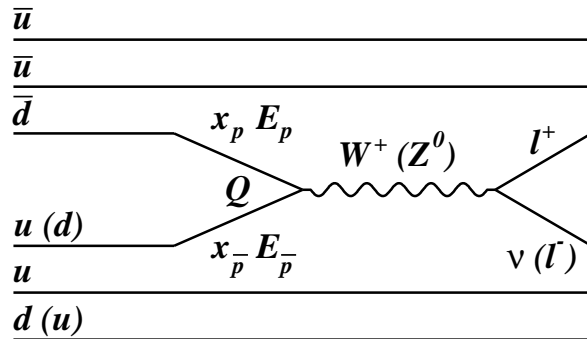


Figure 1: Leading-order production of W and Z bosons at the Tevatron [5]. Additional corrections from initial-state QCD or final-state QED radiation must be modelled accurately for the m_W measurement.

2.1. Parton Distribution Functions

The momentum fraction x of a given colliding parton is described by the parton distribution functions (PDFs). The PDFs are defined and fit to global data by independent groups [11, 12] at a fixed momentum transfer Q , and extrapolated to higher Q using the DGLAP equations [13]. Uncertainties on the input data are typically smaller than the deviations between the data for a given parton distribution function, resulting in poor global values of χ^2 on the fits. Estimates of the PDF uncertainty on any given quantity follow an ad-hoc recipe defined by the fitters. The recipe typically gives a “90% confidence level (C.L.)” uncertainty, though this is based more on experience than on pure statistics. A significant challenge to the m_W measurement is ensuring the accuracy of this uncertainty, and reducing it.

The uncertainty on m_W due to PDFs arises from the detector acceptance to a charged lepton at a given pseudorapidity. Charged leptons decaying transverse to the beam carry the highest p_T (half the boson mass, to first order). The smaller the decay angle with respect to the beam line, the smaller the p_T . At small angles, the charged lepton leaves the detector acceptance, and boosting the lepton along the beam line affects the distribution of angles (and, correspondingly p_T) accepted by the detector. An uncertainty on the boost translates weakly into an uncertainty on m_W . The PDF uncertainty on the most recent DØ (CDF) m_W measurement is 10 (13) MeV [4, 5].

Tevatron data provide significant constraints on PDFs. For the m_W measurement, the most relevant constraints come from measurements of the Z boson rapidity distribution and the W boson production charge asymmetry. Because $\sigma_W \times BR(W \rightarrow \nu\bar{\nu})/\sigma_Z \times BR(Z \rightarrow ll) \approx 10$ [14], the W boson charge asymmetry has greater statistical power than the Z boson rapidity. In addition, the charge asymmetry is a direct study of the W boson production relevant to the m_W measurement.

2.1.1. W Boson Charge Asymmetry

On average, up quarks carry a higher fraction of the proton’s momentum than down quarks. Thus, the longitudinal momentum of the W^+ boson tends to be in the direction of the proton momentum. A measurement of the asymmetry between W^+ and W^- production at a given boson rapidity gives information on the ratio of up- to down-quark momentum fraction. Historically, the asymmetry between the charged leptons from the W boson decay have been measured, since the neutrino is not measured and the W -boson’s rapidity can not be fully reconstructed. The DØ Collaboration has recently performed such a measurement (Fig. 2 [15]), and incorporating its results into the PDF fits will improve their accuracy.

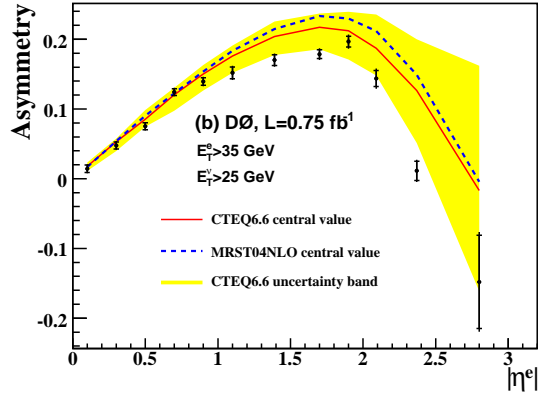


Figure 2: The electron charge asymmetry as a function of pseudorapidity, as measured by the DØ Collaboration (points) and predicted by the CTEQ (solid line) and MRST (dashed line) PDF fits. Also shown is the CTEQ 90% C.L. uncertainty band.

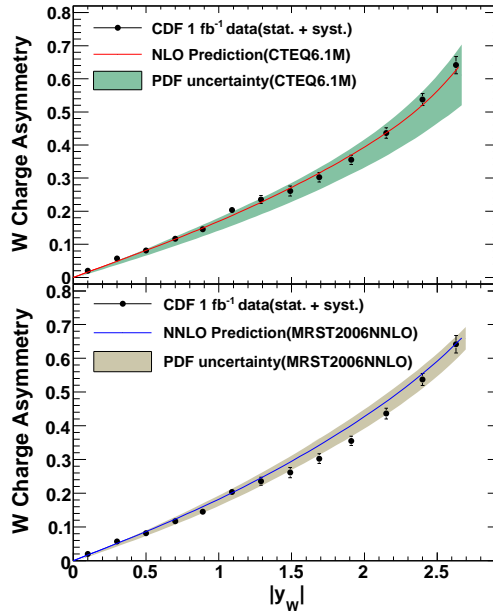


Figure 3: The W boson charge asymmetry as a function of rapidity, as measured by the CDF Collaboration (points) and predicted by the CTEQ (top) and MRST (bottom) fits (including the 90% C.L. uncertainty bands).

The CDF Collaboration has developed a novel method for directly measuring the W -boson charge asymmetry. The method solves for the boson rapidity using the W -boson mass as a constraint. The two solutions are given weights according to the expected boson kinematic and decay distributions. To remove any dependence on the input charge asymmetry, the procedure is iterated until a stable solution is reached. The CDF data (Fig. 3 [16]) will significantly improve predictions of the PDFs at high W boson rapidity.

2.1.2. Issues for the m_W Measurement

With the overall precision on m_W expected to approach 20 MeV in the next iteration of Tevatron measurements, it is useful to consider methods to produce a more robust estimate of the PDF uncertainty. Currently, both CDF and DØ rescale the 90% C.L. uncertainty obtained from the CTEQ recipe to produce a 68% C.L. uncertainty on m_W . This is motivated by the empirical observation that the spread of data for the valence u and d quarks are roughly Gaussian [17]. However, the gluon contribution to the m_W uncertainty is non-negligible, and the 90% C.L. definition is not obtained strictly by statistics. There is thus some ambiguity as to whether the rescaling of uncertainties is appropriate.

In addition to the question of uncertainty scaling, there is the issue of the functions used to parametrize the PDFs. There is considerable flexibility in the choice of functions, and there are various assumptions that are generally made to reduce the number of parameters in the fits. The existence of multiple PDF fits is extremely useful in this regard, and with respect to the definition of the uncertainty, since the various fits use different parametrizations. However, the existing fits are clearly not exhaustive, raising the possibility of an underestimated uncertainty due to a parametrization that poorly describes the distribution function.

There are several possible strategies for obtaining a more robust PDF uncertainty. One can measure m_W using leptons at higher pseudorapidity, though this involves enormous effort to calibrate these detector regions. One can fit for m_W in several lepton pseudorapidity bins to demonstrate that the PDFs accurately describe the distributions within the detector acceptance. Or one can apply an uncertainty obtained strictly (or dominantly) from Tevatron data, which would presumably provide a better χ^2 but a larger uncertainty. At the LHC, the larger statistics and detector coverage will make some of these tests more feasible than at the Tevatron.

2.2. Boson p_T

A majority of W and Z bosons are produced with low p_T (Fig. 4 [5]), where non-perturbative QCD must be used to describe the p_T distribution. Both CDF and DØ model this distribution using the RESBOS generator [18], which is based on a differential calculation with parameters motivated by a resummation calculation in the non-perturbative regime. There are three parameters, g_i ($i = 1, 2, 3$), whose values are constrained by fits to data. The most relevant parameter for the m_W measurement is g_2 , which determines the position of the distribution's peak.

CDF obtains $g_2 = 0.685 \pm 0.048(\text{stat})$ [5] using the $Z \rightarrow ll$ control samples for its m_W measurement. This

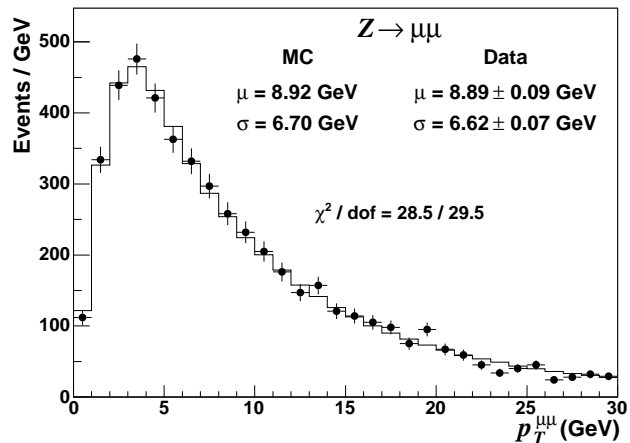


Figure 4: The measured dimuon p_T in 200 pb^{-1} of CDF data, for muon pairs with invariant mass between 66 and 116 GeV.

value of g_2 , which uses CTEQ6M PDFs, is consistent with the value of $g_2 = 0.68_{-0.01}^{+0.02}$ obtained from a global fit using CTEQ3M PDFs. The other g_i parameters are correlated and CDF found that varying g_3 has a negligible effect on m_W .

DØ has performed a dedicated measurement of g_2 for use in its m_W measurement. To maximize sensitivity to g_2 , DØ projects the Z boson p_T along the axis bisecting the charged leptons (Fig. 5). Fitting this distribution in the electron and muon decay channels gives $g_2 = 0.63 \pm 0.02$ using CTEQ6.6 PDFs. DØ has studied the PDF uncertainty on g_2 , finding $\delta g_2(\text{PDF}) = 0.04$.

The crucial step for the m_W measurement is translating the g_2 value obtained by fitting the Z boson p_T into the appropriate value for p_T^W . The RESBOS parametrization provides this translation, but the uncertainty due to higher resummation orders has not been determined. In addition, variations in α_s affect the high end of the p_T spectrum and could cause a small uncertainty on m_W . At the low end of the spectrum, small modifications could arise from QED initial-state radiation, which should be investigated. Other issues relevant to the m_W measurement are including the full correlations with PDFs when determining the uncertainty, and including the diffractive production component that is not modelled by RESBOS.

Starting with the DØ Run 1B m_W measurement [19], the Tevatron experiments have quoted measurements of m_W based on fits to the charged-lepton and neutrino p_T distributions. These fits are more sensitive to the modelling p_T^W than the traditional m_T ($= \sqrt{2p_T^l p_T^\nu (1 - \cos \Delta\phi)}$) fit, providing an important test of the p_T^W model.

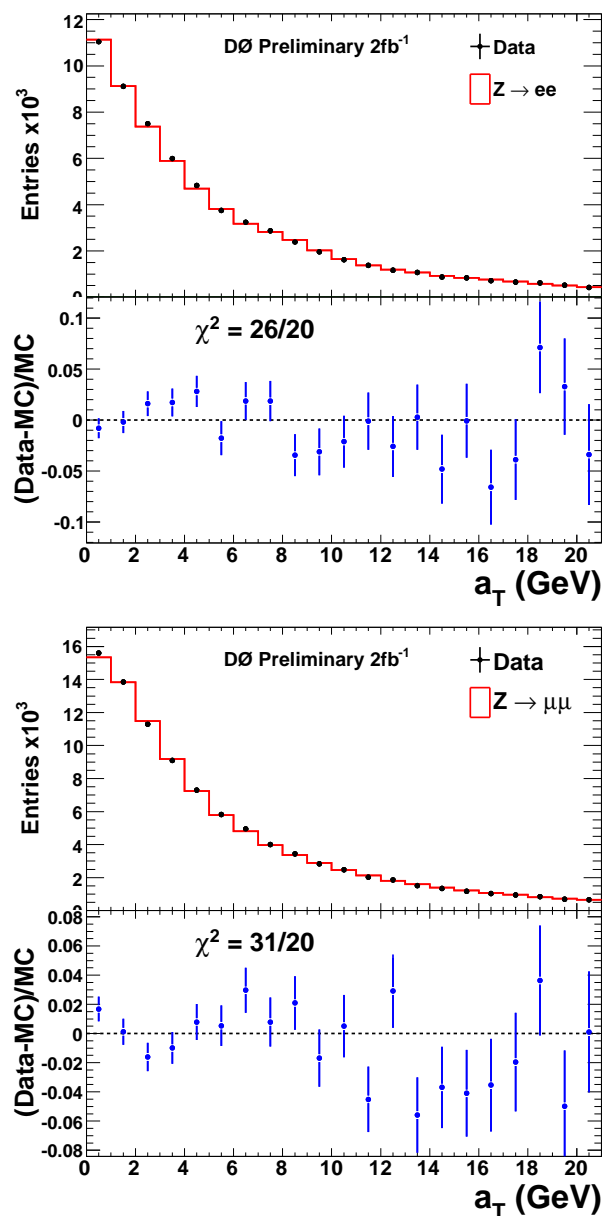


Figure 5: The measured dimuon p_T projected along the axis bisecting the muon pair (a_T), for 2 fb^{-1} of dielectron and dimuon DØ data, and for RESBOS simulation using CTEQ6.6 and $g_2 = 0.63$.

2.3. QED Radiation

Final-state photon radiation (FSR) off a charged lepton from the W boson decay reduces the charged lepton momentum, and thus the inferred boson mass. Modelling this effect results in an $\mathcal{O}(150 \text{ MeV})$ correction to the measured m_W [5]. DØ models FSR with PHOTOS [20], a resummed calculation focused exclusively on FSR, and compares with WGRAD [21], a next-to-leading order (NLO) calculation. CDF uses a histogram of photons extracted from WGRAD to apply FSR at the end of event generation.

To determine the uncertainty on m_W due to the FSR model, DØ takes the difference between fits using PHOTOS and WGRAD. This is almost certainly an overestimate, since PHOTOS includes higher-order terms (through resummation) that WGRAD does not. The uncertainty is nonetheless small due to the electron energy calibration using the Z boson mass, which largely corrects for mismodelling of photon radiation.

CDF models higher-order QED radiation by scaling the photon energy by 10%, taking half the scaling correction as an uncertainty. Other uncertainties due to the infrared cutoff in WGRAD and a comparison of full $\mathcal{O}(\alpha)$ and FSR-only WGRAD are also quoted. CDF is undertaking a thorough investigation of higher-order QED effects using the HORACE generator [22].

HORACE calculates the leading logarithm QED corrections, and reweights them to model the full α^n calculation. The procedure assumes that the reweighting needed to model $\mathcal{O}(\alpha)$ is the same for all orders of α . A CDF study has found that the reweighting produces a $4.5 \pm 1.4 \text{ MeV}$ shift in the m_W fit, when compared to the leading log calculation. A comparison of the reweighted logs with the $\mathcal{O}(\alpha)$ calculation shows an ≈ 10 (20) MeV shift for electrons (muons). The mass shift is lower in the reweighted log simulation, since the higher orders suppress soft QED radiation. Variations in the truncation of the perturbative series in HORACE have less than a 1 MeV effect on m_W .

The HORACE generator improves our understanding of QED radiation, though there is no clear recipe for determining the residual uncertainty on m_W . A full $\mathcal{O}(\alpha^2)$ calculation would be useful in order to validate the HORACE reweighting procedure, but this requires significant effort. Such a calculation could address the question of whether there are uncertainties due to additional diagrams not accounted for in the HORACE reweighting scheme (e.g., final-state radiation of electron-positron pairs). Alternative generators could also be useful; for example, the WINHAC [23] generator incorporates higher orders through exponentiation rather than showering and could provide a cross-check, but not a measure of uncertainty.

Another issue is the potential correlation between initial-state QCD and final-state QED radiation. Currently, CDF and DØ factorize the two, generating QED FSR after RESBOS, or boosting bosons produced by HORACE. Recently, unified generators have become available: the HORACE authors have added MC@NLO [24] for QCD ISR, and the RESBOS authors have added QED FSR in the generator RESBOSA. However, these are still factorized approaches and do not include interference between QCD and QED radiation.

Uncertainties on QED FSR can be mitigated by calibrating the lepton momentum using the Z boson mass in $Z \rightarrow ll$ events. DØ uses this technique for its calibration, though CDF does not because doing so would inflate the overall uncertainty due to the relatively small $Z \rightarrow ll$ statistics.

2.4. Boson Decay

The left-handed coupling of the W boson to the quarks and leptons produces a decay angular distribution proportional to $(1 + \cos \theta)^2$ for production by valence quarks at leading order, where θ is the angle between the (anti)quark and (anti)lepton momenta. Higher-order QCD corrections modify the angular distributions, and have been calculated at NLO and implemented in RESBOS. A comparison of RESBOS to the dedicated NLO generator DYRAD [25] shows consistency in the region of high W boson p_T ($p_T^W > 15$ GeV). At lower p_T the distributions are more accurately described by a resummation procedure, which for RESBOS involves an averaging over helicities. Resummation calculations separated by helicity are in progress, but until they are complete there is some ambiguity of the uncertainty on m_W from the RESBOS decay model.

3. Tevatron m_W Measurements

The CDF and DØ experiments use independent procedures to calibrate the detector response to charged leptons and to hadrons from the underlying event. CDF utilizes its precision tracker to measure m_W in both $W \rightarrow \mu\nu$ and $W \rightarrow e\nu$ decays, while the DØ measurement relies on its hermetic calorimeter to focus on the electron decay channel.

3.1. Charged Lepton Calibration

The CDF lepton momentum calibration begins with the tracker. Charged-track momentum is calibrated using $J/\psi \rightarrow \mu\mu$, $\Upsilon \rightarrow \mu\mu$, and $Z \rightarrow \mu\mu$ events. Fits to the invariant mass of muon pairs in these samples set the momentum scale, and are sensitive to modelling of the ionization energy loss. CDF models the energy loss using the mean from the Bethe-Bloch equation [26] for each traversed layer of material. In the J/ψ sample, which contains more than 600,000 events, the calibration uncertainty is dominated by the energy loss model. Modelling the energy loss as a Landau distribution could improve the quality of the calibration fit, resulting in a smaller overall uncertainty. However, some care is required to preserve the Bethe-Bloch mean when using the Landau distribution.

CDF calibrates the average muon energy loss by fitting the momentum scale as a function of mean inverse transverse momentum of muons from J/ψ decays (Fig. 6). The width of the observed peak is also sensitive to the intrinsic detector resolution and multiple scattering in the detector. The multiple scattering model includes non-Gaussian tails based on data from low-energy muons impinging on a fixed target [27].

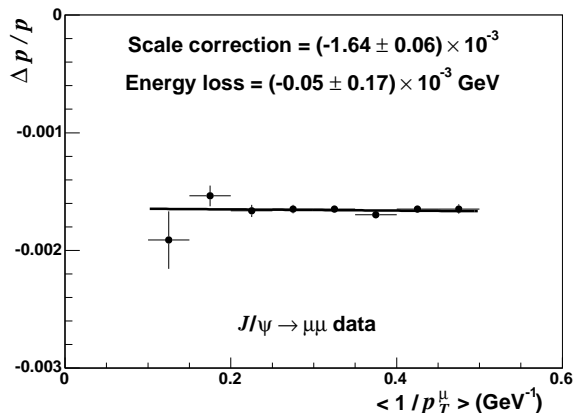


Figure 6: The momentum scale required in the simulation to obtain the world-average J/ψ mass. The scale is plotted as a function of mean inverse p_T of muon pairs from J/ψ decays, and fit to a line where the slope equals the residual energy loss and the intercept equals the momentum scale.

The CDF electron momentum calibration transfers the track calibration to the calorimeter using electrons from W boson decays. CDF fits the ratio of calorimeter energy to track momentum (E/p) using the peak region (Fig. 7). The position of the peak is sensitive to the radiation of low-momentum photons in the tracker. The rate of this radiation is in turn sensitive to the amount of tracker material, which is tuned using the high end of the E/p (1.19 – 1.85) distribution. This tuning empirically corrects the rate of high-momentum radiation, and relies on the theoretical radiation spectrum to model the region near the peak. For very low momentum radiation ($\lesssim 50$ MeV), the model includes quantum-mechanical interference effects that suppress the radiation.

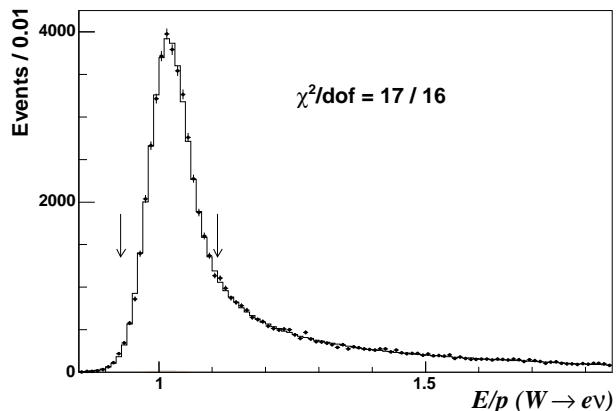


Figure 7: The ratio of calorimeter energy to track momentum for electrons from W boson decays. The region between the arrows is used to fit for the calorimeter energy scale.

CDF tests its lepton momentum calibration by fitting for the Z boson mass using $Z \rightarrow ll$ events. The consistency of the fit m_Z with the LEP measurements [2] in both the electron and muon decay channels provides a stringent test of the detector response and modelling of radiative corrections from first principles. CDF adds the m_Z fit to its momentum calibration, though the relatively low Z boson statistics results in a negligible contribution to the muon calibration, and a 30% contribution to the electron calibration. Since the muon calibration uncertainties are dominantly systematic, it is expected that future measurements will rely more on the Z boson mass fit.

The $D\bar{O}$ electron momentum calibration is based solely on fits to the Z boson mass, as a function of detector region. The calibration determines both the energy scale and an offset. The offset corrects for any inaccuracies in the modelling of detector noise and underlying event in the electron energy measurement. After calibration, the Z boson mass distribution is well described by the simulation (Fig. 8).

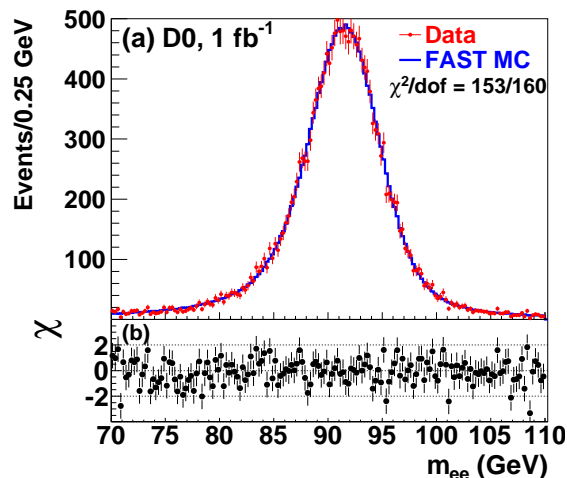


Figure 8: (a) The dielectron mass distribution for 1 fb^{-1} of calibrated $D\bar{O}$ data and simulation. (b) The difference between data and simulation, divided by the expected statistical uncertainty on the data.

The use of $Z \rightarrow ll$ events for calibration cancels a number of systematic uncertainties when applied to the $W \rightarrow l\nu$ mass sample. However, there is no independent test of the calibration, making the measurement less robust and ultimately increasing the overall uncertainty. In addition, extra care must be taken to understand and account for uncertainties that do not cancel when the calibration is applied to the W boson sample. For example, the electron p_T measurement relies on a measurement of the track angle with respect to the beam line. A global scale of this angle that brings the track closer to the beam line can bias the m_Z fit up or down, depending on the topology. However, the m_W fit is always biased to lower values.

3.2. Neutrino Calibration

Since the neutrino momentum is inferred from the measured momentum imbalance of the event, the neutrino calibration is effectively a calibration of all the particles in the event. Excluding the charged lepton from the W boson decay, these particles are known as the recoil. The recoil momentum is the vector sum of diffuse contributions that are not as well measured as the charged lepton (Fig. 9). The detector response to these particles uses an empirical model with parameters determined from $Z \rightarrow ll$ events.

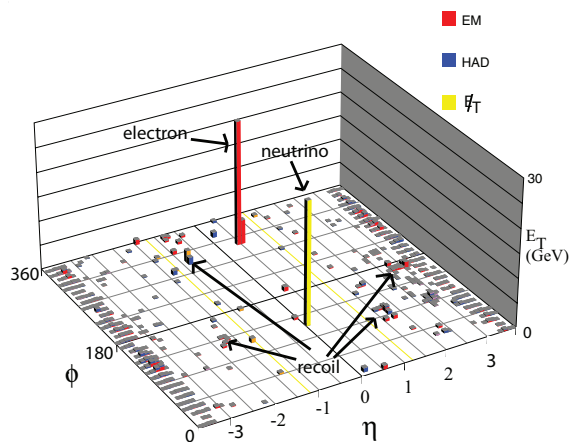


Figure 9: A $W \rightarrow e\nu$ candidate event collected with the $D\bar{O}$ detector. The electron and representative components of the recoil are indicated, as well as the inferred neutrino position and transverse momentum.

The CDF recoil calibration defines a physics-motivated model for the scale and resolution of the recoil. The scale is a logarithmic function of boson p_T . As p_T increases, the particles in the recoil have higher p_T and are contained in a smaller jet cone. The resolution improves with increasing p_T , with the expected dependence of a sampling calorimeter. The resolution due to underlying event uses the same dependence, with parameters determined from data collected with an unbiased trigger. With a few parameters CDF has demonstrated quantitative agreement between data and simulation for the important recoil distributions in the W boson samples. For example, the projection of the recoil vector along the direction of the muon in $W \rightarrow \mu\nu$ events is shown Fig. 10.

The $D\bar{O}$ recoil calibration uses a detector-response library as a function of true recoil momentum, derived using $Z \rightarrow ll$ events and an unbiased trigger to model the effects of the underlying event [28]. The use of a library removes any assumptions on the form of the response functions, though the properties of these functions must be checked to ensure that they are re-

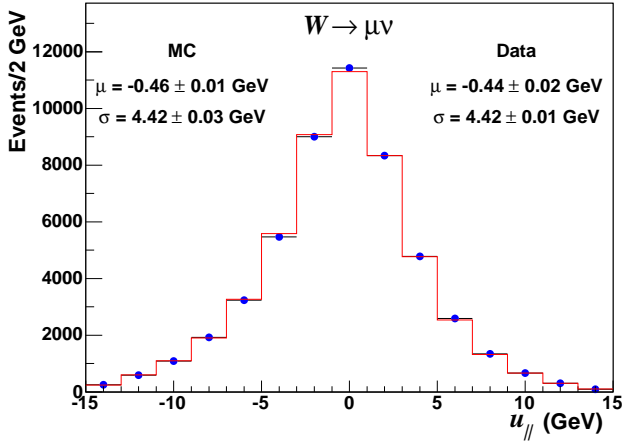


Figure 10: The projection of the recoil vector along the direction of the muon in $W \rightarrow \mu\nu$ events collected by the CDF detector. A bias in the mean of this distribution translates into an equivalent bias on the W boson mass measured using the m_T distribution.

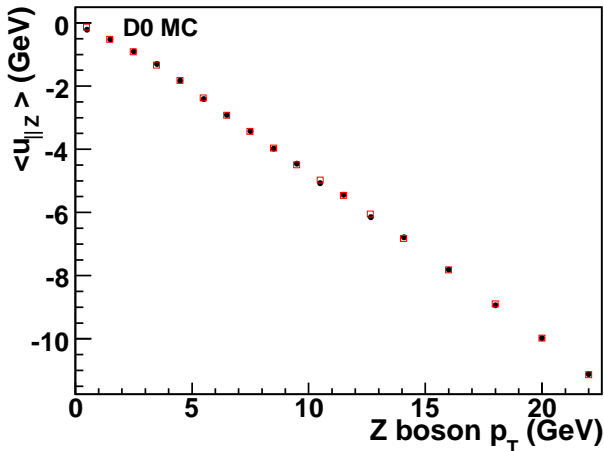


Figure 11: The projection of the recoil vector along the direction of the electrons in $Z \rightarrow ee$ events collected by the DØ detector.

alistic. The DØ model accurately describes the recoil distributions of the calibration sample; as an example, the projection of the observed recoil along the direction of the electrons in $Z \rightarrow ee$ events is shown in Fig. 11. The quality of the model for the W boson recoil distributions has yet to be shown.

3.3. W Boson Mass Fits

Fits for m_W are performed using the charged-lepton and neutrino p_T spectra, and the reconstructed m_T distribution. The latter provides the most precise measurement of m_W , with the combination of the fits improving the total precision by a few percent. The

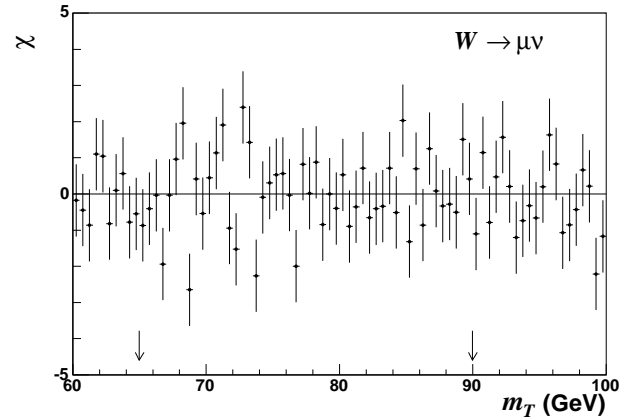
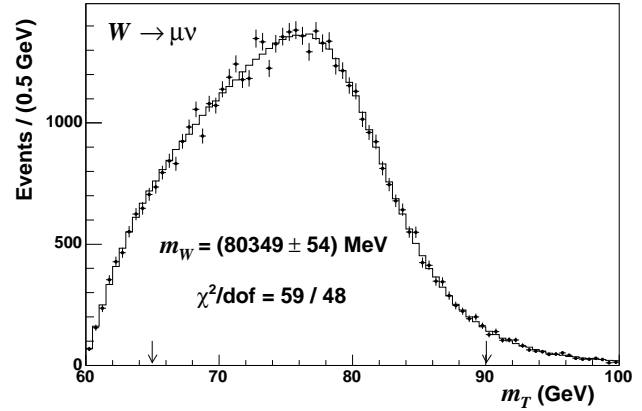


Figure 12: Top: The fit to the m_T spectrum from the $W \rightarrow \mu\nu$ decays measured with the CDF detector. Bottom: The difference between data and simulation, divided by the statistical uncertainty on the expectation.

results of the m_T fits in the muon channel at CDF and the electron channel at DØ are shown in Figs. 12 and 13, respectively.

The CDF and DØ m_W measurements are:

$$m_W = 80.413 \pm 0.034(\text{stat}) \pm 0.034(\text{sys}) \text{ GeV (CDF),}$$

$$m_W = 80.401 \pm 0.021(\text{stat}) \pm 0.038(\text{sys}) \text{ GeV (DØ).}$$

These are the two most precise measurements from individual experiments. The systematic uncertainties on the measurements are shown in Tables II and III. In both cases the dominant uncertainty is on the lepton momentum scale calibration, which is performed in situ. Thus, this uncertainty is expected to reduce with increased statistics.

Combining all Tevatron measurements gives [7]:

$$m_W = 80.420 \pm 0.031 \text{ GeV (Tevatron),} \quad (1)$$

which is more precise than the combined LEP measurement of $m_W = 80.376 \pm 0.033$ GeV. The current world-average value of m_W is [7]

$$m_W = 80.399 \pm 0.023 \text{ GeV (World average).} \quad (2)$$

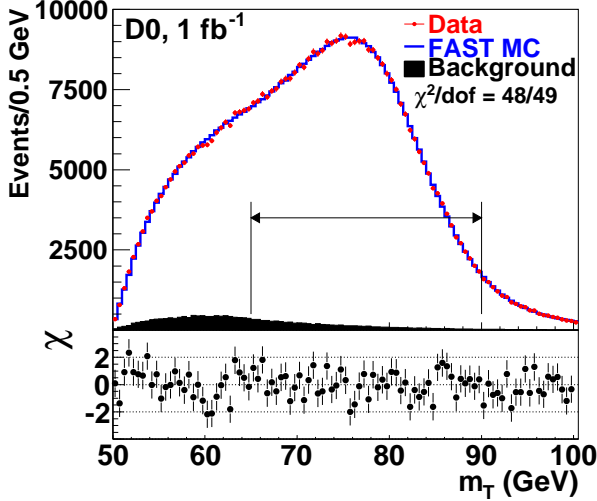


Figure 13: The projection of the recoil vector along the direction of the electrons in $Z \rightarrow ee$ events collected by the DØ detector.

Source	δm_W (MeV)		
	m_T	p_T^e	p_T^ν
Electron energy calibration	34	34	34
Electron resolution model	2	2	3
Electron shower modeling	4	6	7
Electron energy loss model	4	4	4
Hadronic recoil model	6	12	20
Electron efficiencies	5	6	5
Backgrounds	2	5	4
Experimental Subtotal	35	37	41
PDF	10	11	11
QED	7	7	9
Boson p_T	2	5	2
Production Subtotal	12	14	14
Total	37	40	43

Table II Systematic uncertainties on the DØ m_W measurement [4].

4. Global Electroweak Fits

Several groups have updated their fits to the global electroweak data using the latest m_W measurements. The Gfitter group has obtained a best-fit Higgs boson mass $m_H = 83_{-23}^{+30}$ GeV [29], more than 1σ below the LEP direct exclusion $m_H > 114$ GeV [30]. There is thus tension between the electroweak fits and m_H , and this tension increases if one only considers the predictions from m_W alone. The Gfitter group has fit for m_H using only one sensitive variable at a time, and obtains $m_H = 42_{-22}^{+56}$ GeV when using only m_W (Fig. 14). In fact, all measurements prefer a low-mass Higgs, except the forward-backward asymmetry

Source	Uncertainty (MeV)
Lepton Scale	23.1
Lepton Resolution	4.4
Lepton Efficiency	1.7
Lepton Tower Removal	6.3
Recoil Energy Scale	8.3
Recoil Energy Resolution	9.6
Backgrounds	6.4
PDFs	12.6
W Boson p_T	3.9
Photon Radiation	11.6

Table III Systematic uncertainties on the combination of the six fits in the electron and muon channels for the CDF m_W measurement [5].

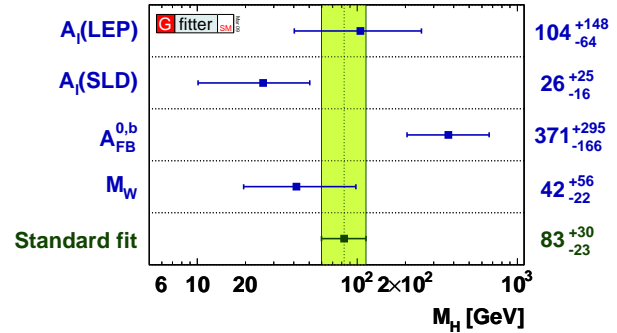


Figure 14: The value of m_H preferred by measurements of the forward-backward lepton asymmetry in e^+e^- collisions at LEP and SLD, the forward-backward b -quark asymmetry at SLD, and the m_W measurement. All variables sensitive to m_H are removed from the fit except for the one quoted [29].

measurement in polarized electron-positron collisions. The Gfitter group has determined the probability of such a deviant measurement to be 1.4%, if due to measurement uncertainties alone.

Given the tension between the electroweak fits and the direct limit on m_H , it is natural to consider possible new-physics contributions to m_W . One possibility is the presence of supersymmetric-particle loops in the W boson propagator. Such loops in the minimal supersymmetric standard model increase the W -boson mass and reduce this tension. Figure 15 shows the range of top-quark and W -boson masses preferred by the MSSM and by the SM [31]. However, there are other constraints on supersymmetry that create a different set of tensions.

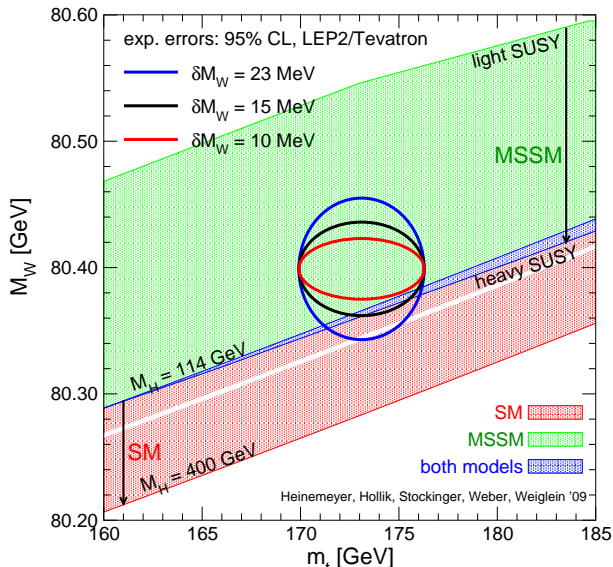


Figure 15: The 95% ellipse for the measured values of m_W and m_t (blue circle), and smaller ellipses for future m_W uncertainties of 15 MeV (black circle) and 10 MeV (red circle) [31]. An uncertainty of 10 MeV would exclude values of the SM Higgs above the current direct lower limit of 114 GeV.

5. Future Measurements

In addition to the expected improvement in m_W precision from analysis of the complete Tevatron datasets, even greater precision is predicted by the ATLAS experiment at the LHC. With 10 fb^{-1} of $\sqrt{s} = 14 \text{ TeV}$ data (one year of running at design luminosity), the ATLAS experiment expects to have a precision of 7 MeV on its measurement of m_W [8]. However, there are significant challenges to achieving this goal. For example, the ATLAS projection is based on the charged-lepton p_T fit for a single decay channel and assumes the recoil uncertainty is negligible. However, both the CDF and DØ measurements find a larger recoil uncertainty on this mass fit than on the fit to the m_T distribution, due to the tight cut on the recoil momentum in the event selection. Thus, one would expect a non-negligible recoil uncertainty for the ATLAS measurement. In addition, ATLAS expects the p_T^W uncertainty to dominate the production model uncertainty, with a negligible PDF uncertainty. Given the large uncertainties on the PDFs at the momentum fraction relevant for W boson production at the LHC, this projection appears optimistic.

Even though there will be significant challenges to overcome for measuring m_W at ATLAS and CMS, there will be $\mathcal{O}(10^8)$ W - and $\mathcal{O}(10^7)$ Z -boson events to calibrate the detector response to leptons and recoil, and to measure the Z boson rapidity and p_T distributions to constrain the PDFs and p_T^W . In addition, there is a W boson charge asymmetry at the LHC

which is similar to that of the Tevatron, providing further possible PDF constraints. Given these large statistics and calibration tools, it is realistic to expect a measurement with precision better than 10 MeV from the LHC experiments.

Finally, there is potential for a precision measurement of the weak mixing angle from the forward-backward asymmetry of leptons in Drell-Yan production at the Tevatron. The distribution of the angle θ between the negative-lepton and proton momenta has the form [32]:

$$d\sigma/d\cos\theta \propto 3/8(1 + \cos^2\theta) + A_{FB}\cos\theta, \quad (3)$$

where A_{FB} is the asymmetry between negative leptons produced in the forward ($\cos\theta > 0$) and backward ($\cos\theta < 0$) directions, and is a function of the vector and axial couplings of the fermions to the Z and γ bosons. Since the vector coupling is equal to $I_L^3 - 2e\sin^2\theta_W$, where I_L^3 is the weak charge, the measurement provides sensitivity to the weak mixing angle.

CDF and DØ have performed measurements of A_{FB} in the electron decay channel with 72 pb^{-1} [32] and 1.1 fb^{-1} [3] of data, respectively. Assuming statistical scaling of the uncertainties on the DØ measurement,

$$\sin^2\theta_W = 0.2326 \pm 0.0018(\text{stat}) \pm 0.006(\text{sys}), \quad (4)$$

the combined Tevatron precision using electron and muon channels in $\mathcal{O}(10) \text{ fb}^{-1}$ of data could approach 0.0003, which would contribute to the world-average value of $\sin^2\theta_W = 0.23149 \pm 0.00013$.

6. Conclusions

The model of electroweak unification has been tested to high precision, and is now used to constrain the existence and properties of unobserved particles coupling to the W and Z bosons. Further progress relies on improving the measurement of the W boson mass, whose uncertainty is the limiting factor in these constraints. Measurements at the Tevatron have recently reduced this uncertainty significantly, with further reduction expected from analysis of the existing data. In order to achieve the stated goal of a measurement more precise than the current world average, the Tevatron experiments require improvements in the model of W and Z boson production. Ongoing theoretical work and recent production measurements should produce the needed improvements. Ultimately, the LHC should produce a measurement of m_W with better than 10 MeV precision. At that point, other uncertainties on parameters in the electroweak fits will need to be revisited, for example the uncertainty on the electromagnetic coupling α , evaluated at the Z boson mass.

Another possibility for improving electroweak constraints is the determination of $\sin^2 \theta_W$ through the measurement of the forward-backward asymmetry of Drell-Yan at the Tevatron. However, much work is required to demonstrate the scaling of uncertainties with an order of magnitude more data, and to achieve sensitivity in the muon decay channel.

Overall, there is significant ongoing progress in precision electroweak measurements at hadron colliders. The constraints on the Higgs boson mass are quickly tightening, and if there is no SM Higgs there is a reasonable possibility that it will be first excluded by the W boson mass measurement.

Acknowledgments

I would like to thank the Electroweak session conveners, Ashutosh Kotwal, Uli Baur, and Tim Bolton, for inviting me to give this review, and for providing useful comments on these proceedings.

References

- [1] S. Glashow, Nucl. Phys. **22**, 579 (1967); S. Weinberg, Phys. Lett. **12**, 132 (1967); A. Salam, *Elementary Particle Physics*, N. Svartholm ed., 367 (1968).
- [2] S. Schael *et al.* (ALEPH, DELPHI, L3, OPAL, and SLD Collaborations), Phys. Rep. **427**, 257 (2006).
- [3] V. M. Abazov *et al.* (DØ Collaboration), Phys. Rev. Lett. **101**, 191801 (2008).
- [4] V. M. Abazov *et al.* (DØ Collaboration), Phys. Rev. Lett. **103**, 141801 (2009); V. M. Abazov *et al.* (DØ Collaboration), *arXiv:0909.4814v1* (2009).
- [5] T. Aaltonen *et al.* (CDF Collaboration), Phys. Rev. D **77**, 112001 (2008); T. Aaltonen *et al.* (CDF Collaboration), Phys. Rev. Lett. **100**, 071801 (2008); T. Aaltonen *et al.* (CDF Collaboration), Phys. Rev. Lett. **99**, 151801 (2007).
- [6] The Tevatron Electroweak Working Group, *arXiv:0903.2503v1* (2009).
- [7] The Tevatron Electroweak Working Group, *arXiv:0908.1374v1* (2009).
- [8] N. Besson *et al.*, Eur. Phys. J. C **57**, 627 (2008); G. Aad *et al.* (ATLAS Collaboration), *arXiv:0901.0512* (2009).
- [9] D. C. Kennedy and B. W. Lynn, Nucl. Phys. B **322**, 1 (1989); M. B. Einhorn, D. R. T. Jones, and M. Veltman, Nucl. Phys. B **191**, 146 (1981).
- [10] M. Awramik, M. Czakon, A. Freitas, and G. Weiglin, Phys. Rev. D **69**, 053006 (2004).
- [11] A. D. Martin, R. G. Roberts, W. J. Stirling, and R. S. Thorne, Eur. Phys. J. C **28**, 455 (2003).
- [12] J. Pumplin *et al.*, J. High Energy Phys. **0207**, 012 (2002).
- [13] V. N. Gribov and L. N. Lipatov, Sov. J. Nucl. Phys. **15**, 438 (1972); G. Altarelli and G. Parisi, Nucl. Phys. B **126**, 298 (1977); Y. L. Dokshitzer, Sov. Phys. JETP **48**, 641 (1977).
- [14] A. Abulencia *et al.* (CDF Collaboration), J. Phys. G **34**, 2457 (2007).
- [15] V. M. Abazov *et al.* (DØ Collaboration), Phys. Rev. Lett. **101**, 211801 (2008).
- [16] T. Aaltonen *et al.* (CDF Collaboration), Phys. Rev. Lett. **102**, 181801 (2009).
- [17] J. M. Campbell, J. W. Huston, and W. J. Stirling, Rep. Prog. Phys. **70**, 89 (2007).
- [18] F. Landry, R. Brock, P.M. Nadolsky, and C.-P. Yuan, Phys. Rev. D **67**, 073016 (2003); C. Balazs and C.-P. Yuan, Phys. Rev. D **56**, 5558 (1997); G. A. Ladinsky and C.-P. Yuan, Phys. Rev. D **50**, R4239 (1994).
- [19] B. Abbott *et al.* (DØ Collaboration), Phys. Rev. D **58**, 092003 (1998).
- [20] E. Barbiero and Z. Was, Comput. Phys. Commun. **79**, 291 (1994).
- [21] U. Baur, S. Keller, and D. Wackerroth, Phys. Rev. D **59**, 013002 (1998).
- [22] C. M. Carloni Calame *et al.*, Phys. Rev. D **69**, 037301 (2004).
- [23] W. Placzek and S. Jadach, Eur. Phys. J. C **29**, 325 (2003).
- [24] S. Frixione and B. R. Webber, J. High Energy Phys. **0206**, 029 (2002).
- [25] W. T. Giele, E. W. N. Glover, and D. A. Kosower, Nucl. Phys. B **403**, 633 (1993).
- [26] W.-M. Yao *et al.*, J. Phys. G **33**, 1 (2006).
- [27] D. Attwood *et al.* (MuScat Collaboration), Nucl. Instrum. Methods Phys. Res. B **251**, 41 (2006).
- [28] V. M. Abazov *et al.* (DØ Collaboration), Nucl. Instrum. Methods Phys. Res. A **609**, 250 (2009).
- [29] H. Flücher *et al.* (The Gfitter Group), Eur. Phys. J. C **60** 543 (2009).
- [30] R. Barate *et al.* (ALEPH Collaboration, DELPHI Collaboration, L3 Collaboration, OPAL Collaboration, and the LEP Working Group for Higgs Boson Searches), Phys. Lett. B **565**, 61 (2003).
- [31] S. Heinemeyer *et al.*, J. High Energy Phys. **08**, 052 (2006).
- [32] D. Acosta *et al.* (CDF Collaboration), Phys. Rev. D **71**, 052002 (2008).